Available online at www.sciencedirect.com
SCIENCE DIRECT®
Journal of Power Sources 119–121 (2003) 156–160
JOURNAL OF POWER SOURCES
www.elsevier.com/locate/jpowsour

Lithium insertion material of $LiNi_{1/2}Mn_{1/2}O_2$ for advanced lithium-ion batteries

Yoshinari Makimura, Tsutomu Ohzuku*

Electrochemistry and Inorganic Chemistry Laboratory, Department of Applied Chemistry, Graduate School of Engineering, Osaka City University (OCU), Sugimoto 3-3-138, Sumiyoshi, Osaka 558-8585, Japan

Abstract

Lithium nickel manganese oxide of $LiNi_{1/2}Mn_{1/2}O_2$, which is a one-to-one mixture of $LiNiO_2$ and $LiMnO_2$ in its chemical composition, has been prepared by an improved processing method. Cycle tests of a lithium cell with $LiNi_{1/2}Mn_{1/2}O_2$ operated in voltages of 2.5–4.5 V shows about 200 mAh g^{-1} of rechargeable capacity without noticeable loss during 30 cycles. The thermal behavior of fully charged $LiNi_{1/2}Mn_{1/2}O_2$ is also examined by differential scanning calorimetry (DSC) and shows that the exothermic reaction of $\square_{0.89}Li_{0.11}Ni_{1/2}Mn_{1/2}O_2$ (fully charged state under this experimental condition) is milder than that of $\square NiO_2$ or $\square Mn_2O_4$. The results on rate-capability tests of a $Li/LiNi_{1/2}Mn_{1/2}O_2$ cell show that 85% of discharge capacity observed at low rate discharge can be stored and delivered at 1 h rate at present.

Keywords: Lithium-ion battery; Lithium nickel manganese oxide; Nickel manganese double hydroxide

1. Introduction

Lithium nickel manganese oxides have been of great interest among material chemists for advanced lithium-ion batteries [1–12]. Of these, $LiNi_{1/2}Mn_{1/2}O_2$ is the most attractive material [2]. In the previous paper [4], we have reported the preliminary results on $LiNi_{1/2}Mn_{1/2}O_2$. It was difficult to prepare battery-active $LiNi_{1/2}Mn_{1/2}O_2$ until the chemical mismatch between $LiNiO_2$ [13,14] and $LiMnO_2$ [15–18] in their processing methods was adjusted. A major breakthrough in this problem was to use nickel manganese double hydroxides, i.e. one-to-one solid solutions of $Ni(OH)_2$ and $Mn(OH)_2$, which have the same crystal structure. Manganese ions in nickel manganese double hydroxides are easily oxidized when wet, so that manganese oxide contamination in the double hydroxide may lead to a structural impurity in $LiNi_{1/2}Mn_{1/2}O_2$. After analytical work using TG/DTA, SEM, XRD and electrochemical examination, we have partially succeeded in improving the material in terms of rechargeable capacity, rate capability, and cycleability.

In this paper, we report on the structural and electrochemical properties of $LiNi_{1/2}Mn_{1/2}O_2$ prepared by an improved processing method.

2. Experimental

The starting material is a nickel manganese double hydroxide with an exact one-to-one ratio of Ni and Mn (MX-014-3; Ni:Mn = 1.005:0.995 in molar ratio) obtained from Tanaka Chemical Corp., Japan. The double hydroxide was dehydrated at 400 °C and a nickel manganese double oxide was obtained. $LiNi_{1/2}Mn_{1/2}O_2$ was prepared by heating a reaction mixture of LiOH and the double oxide at 1000 °C in air. The samples were characterized by XRD (XD-3A, Shimadzu Co., Ltd.) with Cu Kα radiation. The system was equipped with a diffracted graphite monochromator.

Electrochemical cells used were the same as described previously [14]. Positive electrodes were prepared by casting a slurry of 88 wt.% $LiNi_{1/2}Mn_{1/2}O_2$, 6 wt.% acetylene black, and 6 wt.% PVdF dispersed in *N*-methyl-2-pyrrolidone (NMP) on an aluminum foil with a blade. NMP was evaporated at room temperature in air and then under vacuum at 60 °C for 30 min, and finally the electrodes (15 mm × 20 mm) were dried under vacuum at 150 °C for 14 h. Lithium metal was used as a negative electrode (15 mm × 20 mm). Two sheets of polypropylene microporous membrane (Celgard 2500) were used as a separator. Electrolyte was 1 M $LiPF_6$ dissolved in ethylene carbonate (EC)/dimethyl carbonate (DMC) (3/7 v/v) solution. In fabricating the cells, all materials except the electrolyte and lithium metal were dried under vacuum at 60 °C for at least 2 h to avoid possible contamination of water. For the

* Corresponding author.
E-mail address: ohzuku@a-chem.eng.osaka-cu.ac.jp (T. Ohzuku).

0378-7753/03/$ – see front matter
doi:10.1016/S0378-7753(03)00170-8

electrochemical tests the current applied to the cell was 0.5 mA, which corresponds to a current density of 0.17 mA cm^{-2} unless otherwise noted.

For the differential scanning calorimetry (DSC) measurements, $LiNi_{1/2}Mn_{1/2}O_2$ was oxidized in lithium cells, for which $LiNi_{1/2}Mn_{1/2}O_2$ powder was pressed into a pellet without the addition of any carbon or binder and used as a positive electrode. After constant-current charge at 0.17 mA cm^{-2} a pellet was taken out of the cell, and the electrolyte of 1 M $LiPF_6$ EC/DEC (1/1 v/v) was wiped off with a filter paper. A piece of crushed pellet was mechanically sealed in an aluminum cell. The weight of the sample loaded in an aluminum cell including the electrolyte was estimated by weighing the aluminum cells with and without the sample. The DSC signals, a heat flow in mW g^{-1} as a function of temperature, were measured at a heating and cooling rate of 5 °C min^{-1}. Other sets of experimental conditions are given in Section 3.

3. Results and discussion

Fig. 1 shows the XRD patterns of $LiNi_{1/2}Mn_{1/2}O_2$, $LiNiO_2$, and Li_2MnO_3. Li_2MnO_3 can be identified as a layered structure, i.e. $Li[Li_{1/3}Mn_{2/3}]O_2$, while it is distorted to a monoclinic lattice. As seen in Fig. 1(b), well-crystallized $LiNi_{1/2}Mn_{1/2}O_2$ can be prepared by heating the reaction mixture at 1000 °C. All diffraction lines can be indexed by assuming a hexagonal lattice. Lattice parameters obtained for 11 $LiNi_{1/2}Mn_{1/2}O_2$ samples showing the identical electrochemical reactivity with that reported here were

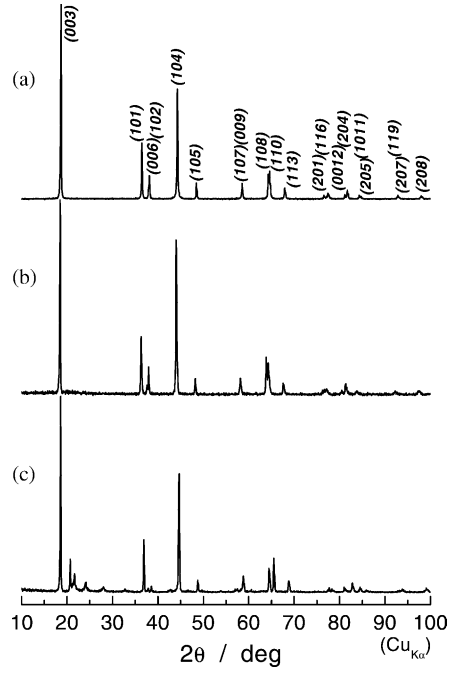

Fig. 1. X-ray diffraction patterns of (a) $LiNiO_2$, (b) $LiNi_{1/2}Mn_{1/2}O_2$, and (c) Li_2MnO_3 ($Li[Li_{1/3}Mn_{2/3}]O_2$).

determined to be $a = 2.891(2)$ Å and $c = 14.30(1)$ Å in a hexagonal setting. The parameters for each sample were obtained by a least squares method using 15 diffraction lines. Batch-to-batch variations of lattice parameters are $a = 2.888$–2.897 Å and $c = 14.289$–14.315 Å for 11 samples. The c-axis dimension is above 14.25 Å, which is the largest value among the layered $LiMeO_2$ (Me: transition metal ions) as far as we know. As can be seen in Fig. 1, the XRD pattern of $LiNi_{1/2}Mn_{1/2}O_2$ is closely related to that of $LiNiO_2$, not to that of $Li[Li_{1/3}Mn_{2/3}]O_2$ having a distorted layered structure. However, the strongest integrated intensity is the (1 0 4) line among the diffraction lines for $LiNi_{1/2}Mn_{1/2}O_2$, not the (0 0 3) line, and the ratio $I_{(0\,0\,3)}/I_{(1\,0\,4)}$ is observed to be 0.85. When we try to optimize the structure of $LiNi_{1/2}Mn_{1/2}O_2$ assuming a space group of $R\bar{3}m$, 8–10% of displacement between the transition metal ions at the 3(a) sites and lithium ions at the 3(b) sites is necessary to adjust the intensities. A battery-active form cannot be expected for a $LiNi_{1/2}Mn_{1/2}O_2$ that consists of highly concentrated rock-salt domains in a $LiNiO_2$-structure as was discussed in detail [14].

The morphology of particles observed by SEM is shown in Fig. 2. The particles re-crystallized at the heating temperature of 1000 °C, and non-porous bodies with a smooth crystal surface can be seen.

Fig. 3 shows the charge and discharge curves of lithium cells with $LiNi_{1/2}Mn_{1/2}O_2$ operated in different voltage ranges at 0.17 mA cm^{-2}. As shown in Fig. 3(c), when the charge-end voltages were set to 5.0 V, the first charge capacity was 245 mAh g^{-1} based on $LiNi_{1/2}Mn_{1/2}O_2$ sample weight, and the first discharge capacity was 215 mAh g^{-1}. About 30 mAh g^{-1} of charge capacity was lost during the first charge and discharge. For subsequent cycles, the rechargeable capacity was about 210 mAh g^{-1} with about 99% of charge–discharge coulombic efficiency. When the cell was operated 2.5–4.3 V, 170 mAh g^{-1} of rechargeable capacity was observed after the first cycle as seen in Fig. 3(a). Fig. 3(b) shows the charge and discharge curves of a Li/$LiNi_{1/2}Mn_{1/2}O_2$ cell operated 2.5–4.5 V, in which the rechargeable capacity was observed to be about 200 mAh g^{-1}. The charge and discharge

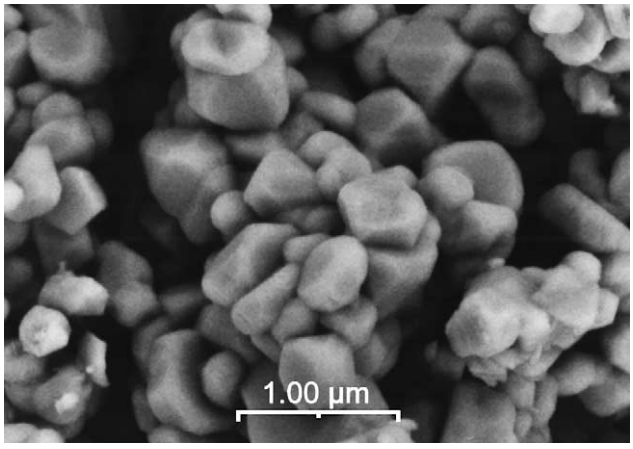

Fig. 2. A SEM photograph of $LiNi_{1/2}Mn_{1/2}O_2$.

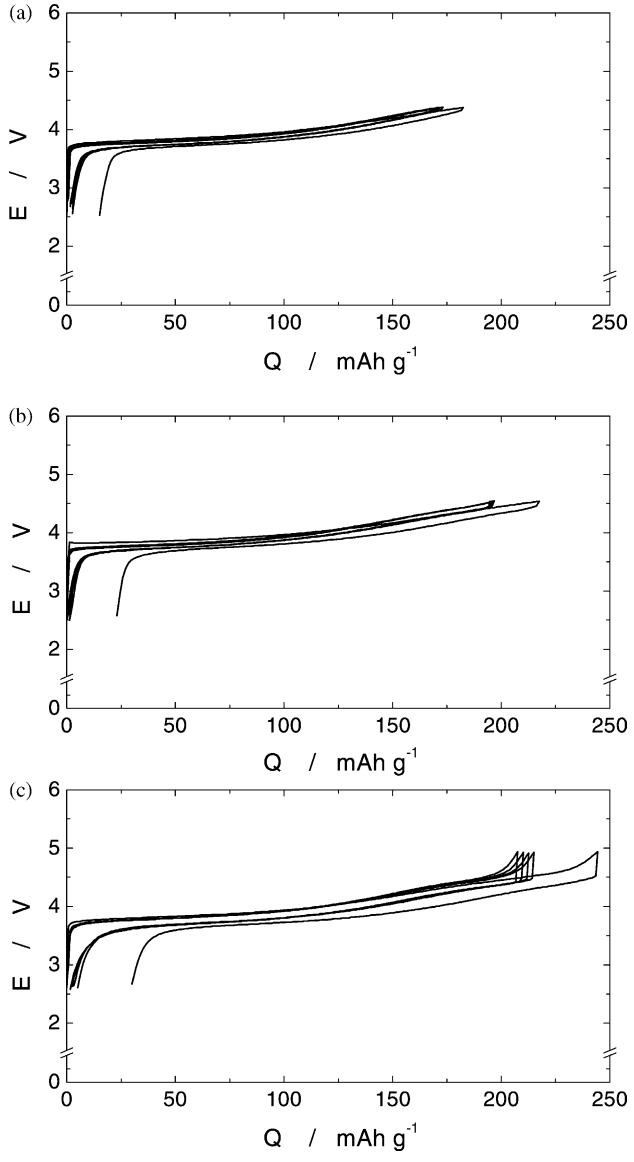

Fig. 3. Charge and discharge curves of a Li/$LiNi_{1/2}Mn_{1/2}O_2$ cell operated in voltages of (a) 2.5–4.3 V, (b) 2.5–4.5 V, and (c) 2.5–5.0 V at a rate of 0.17 mA cm^{-2} at 30 °C.

coulombic efficiencies are more than 99%. For the materials, as with $LiCoO_2$, $LiNiO_2$, and so forth [14,19,20], the rechargeable capacity faded rapidly when they were operated in such a high voltage region.

In order to examine the electrochemical reactivity and stability of $LiNi_{1/2}Mn_{1/2}O_2$, 30-cycle tests were carried out at low-rates. This is one of the most severe operating conditions, because the material was exposed to potentials above 4 V for a long time. As can be seen in Figs. 4 and 5, the Li/$LiNi_{1/2}Mn_{1/2}O_2$ cells show about 200 mAh g^{-1} of rechargeable capacity without dramatic capacity fading during 30 cycles.

Thermal behavior in the partially or fully charged state with electrolyte solution is a key in considering positive-electrode materials for advanced lithium-ion batteries in addition to material stability at high voltage [21]. In order to examine the thermal behavior of lithium nickel manganese oxides, the DSC measurements of $Li_{1-x}Ni_{1/2}Mn_{1/2}O_2$ ($0 \leq x < 1$) containing electrolyte were carried out. Fully charged $LiNi_{1/2}Mn_{1/2}O_2$ were prepared by the electrochemical oxidation of $LiNi_{1/2}Mn_{1/2}O_2$ without the addition of acetylene black and binder in non-aqueous lithium cells. The degree of oxidation was calculated from charge capacity and a theoretical capacity (280 mAh g^{-1}) based on one-electron transfer per a formula unit of $LiNi_{1/2}Mn_{1/2}O_2$. A result on $\square_{0.89}Li_{0.11}Ni_{1/2}Mn_{1/2}O_2$ (250 mAh g^{-1} of charge capacity) is shown in Fig. 6. The DSC curves for $\square NiO_2$ and $\square Mn_2O_4$ with the electrolyte are also shown for comparison. Both samples were chemically prepared by reacting $LiNiO_2$ or $LiMn_2O_4$ with 1 M HNO_3 at room temperature. We confirmed that almost all the lithium ions were extracted from both samples by XRD and TG. As seen in Fig. 6(a), $\square NiO_2$ shows an exothermic peak at 220 °C and an exothermic spike at 210 °C due to the reaction of organic electrolyte

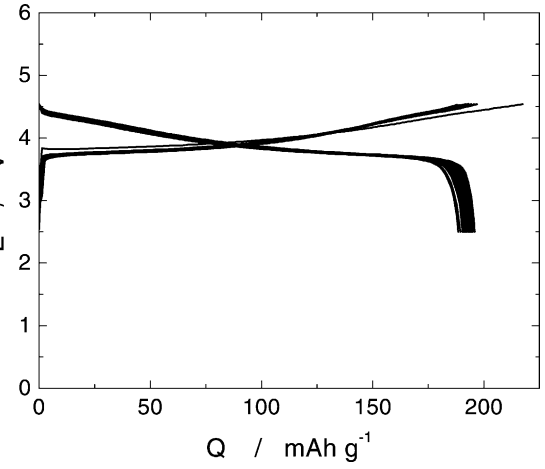

Fig. 4. Charge and discharge curves of a Li/$LiNi_{1/2}Mn_{1/2}O_2$ cell operated in voltages of 2.5–4.5 V at a rate of 0.17 mA cm^{-2} for 30 cycles.

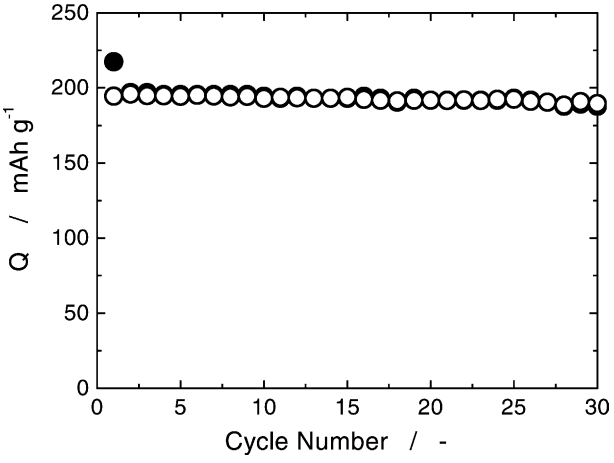

Fig. 5. Charge and discharge capacities as a function of cycle number for a cell operated in voltages of 2.5–4.5 V as shown in Fig. 4. Closed and open circles indicate charge and discharge capacities, respectively.

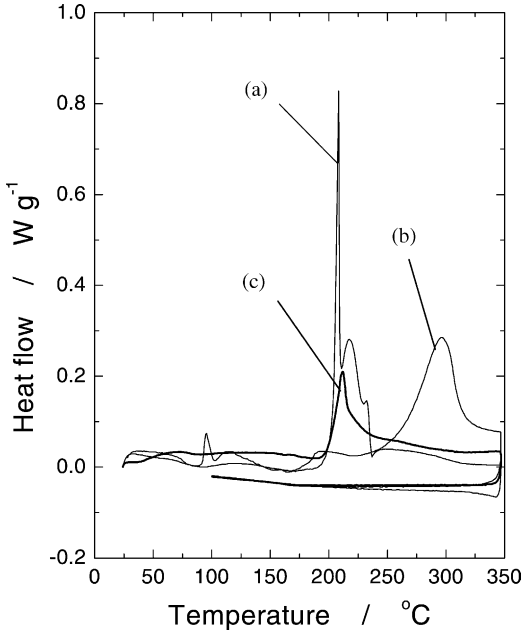

Fig. 6. DSC curves for (a) □NiO_2, (b) □Mn_2O_4 and (c) □$_{0.89}Li_{0.11}Ni_{1/2}Mn_{1/2}O_2$ containing electrolyte of 1 M $LiPF_6$ dissolved in EC/DEC (1/1 v/v). A heating and cooling rate was 5 °C min^{-1}.

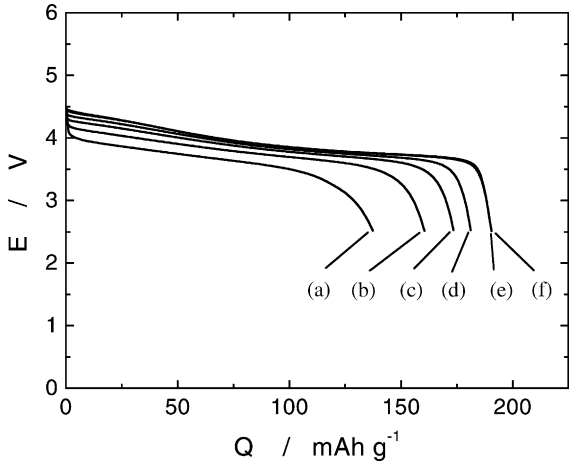

Fig. 7. Rate-capability tests on a Li/$LiNi_{1/2}Mn_{1/2}O_2$ cell. The cell was charged at 0.17 mA cm^{-2} to 4.5 V and then held at 4.5 V for 19 h, and discharged at (a) 6.00 mA cm^{-2} (397.2 mA g^{-1} based on $LiNi_{1/2}Mn_{1/2}O_2$ sample weight), (b) 3.00 mA cm^{-2} (198.6 mA g^{-1}), (c) 1.50 mA cm^{-2} (99.3 mA g^{-1}), (d) 0.75 mA cm^{-2} (49.7 mA g^{-1}), (e) 0.30 mA cm^{-2} (19.9 mA g^{-1}), or (f) 0.17 mA cm^{-2} (11.0 mA g^{-1}).

with □NiO_2. For □Mn_2O_4 an exothermic peak was observed at 300 °C. For fully charged $LiNi_{1/2}Mn_{1/2}O_2$, the exothermic peak is much smaller than those of □NiO_2 and □Mn_2O_4 although the exothermic peak is almost the same temperature as that observed for □NiO_2.

Fig. 7 shows the results on rate-capability tests of a Li/$LiNi_{1/2}Mn_{1/2}O_2$ cell. Discharge currents were varied from 0.17 to 6 mA cm^{-2}, which corresponds to the values of 11–397 mA g^{-1} based on the $LiNi_{1/2}Mn_{1/2}O_2$ sample weight. In other words, rate-capability tests were done for various currents ranging from 18 (1/18*C* rate) to 0.5 h rate (2*C* rate). In calculating *C*-rate, a rechargeable capacity of 200 mAh g^{-1} is assumed to be roughly equivalent to a nominal capacity in a battery technology field. As can be seen in these figures, $LiNi_{1/2}Mn_{1/2}O_2$ is improved by this method in terms of rate capability and rechargeable capacity compared to the results on $LiNi_{1/2}Mn_{1/2}O_2$ prepared by a previous method [2,4].

In this paper, we have focused on the synthesis and electrochemical characterization of $LiNi_{1/2}Mn_{1/2}O_2$ for advanced batteries. At present, the operating voltage of a Li/$LiNi_{1/2}Mn_{1/2}O_2$ cell is a little bit higher than that of a Li/$LiCo_{1/3}Ni_{1/3}Mn_{1/3}O_2$ [3]. As far as these lithium insertion materials are concerned, similarities and differences can be seen in their electronic and crystal structures, which will be presented in separate papers in near future. We believe that $LiNi_{1/2}Mn_{1/2}O_2$ will show higher capacity between 3.5 and 4.35 V versus Li than any other material reported so far, including $LiCo_{1/3}Ni_{1/3}Mn_{1/3}O_2$, if $LiNi_{1/2}Mn_{1/2}O_2$ is well understood, designed and processed.

Acknowledgements

One of us (T.O.) wishes to thank Mr. Hiroyuki Ito of Tanaka Chemical Corp. for his help on the preparation of nickel manganese hydroxide. The present work was partially supported by a grant-in-aid from the Osaka City University Science Foundation.

References

[1] E. Rossen, C.D.W. Jones, J.R. Dahn, Solid State Ion. 57 (1992) 311.
[2] Y. Makimura, T. Ohzuku, in: Proceedings of the 41st Battery Symposium, Abstract no. 2D20–2D21, Nagoya, 2000.
[3] T. Ohzuku, Y. Makimura, Chem. Lett. (2001) 642.
[4] T. Ohzuku, Y. Makimura, Chem. Lett. (2001) 744.
[5] Z. Lu, D.D. MacNeil, J.R. Dahn, Electrochem. Solid-State Lett. 4 (2001) A191.
[6] J.-S. Kim, C.S. Johnson, M.M. Thackeray, Electrochem. Commun. 4 (2002) 205.
[7] C.S. Johnson, J.-S. Kim, A.J. Kropf, A.J. Kahaian, J.T. Vaughey, M.M. Thackeray, Electrochem. Commun. 4 (2002) 492.
[8] B. Ammundsen, J.M. Paulsen, Adv. Mater. 13 (2001) 943.
[9] B.J. Neudecker, R.A. Zuhr, B.S. Kwak, J.B. Bates, J.D. Robertson, J. Electrochem. Soc. 145 (1998) 4148.
[10] Q. Zhong, A. Banakdorpour, M. Zhang, Y. Gao, J.R. Dahn, J. Electrochem. Soc. 144 (1997) 205.
[11] T. Ohzuku, K. Ariyoshi, S. Yamamoto, Y. Makimura, Chem. Lett. (2001) 1270.
[12] T. Ohzuku, K. Ariyoshi, S. Yamamoto, J. Ceram. Soc. Jpn. 5 (2002) 501.
[13] J.R. Dahn, U. von Sacken, C.A. Michal, Solid State Ion. 44 (1990) 87.
[14] T. Ohzuku, A. Ueda, M. Nagayama, J. Electrochem. Soc. 140 (1993) 1862.
[15] T. Ohzuku, A. Ueda, T. Hirai, Chem. Express 7 (1992) 193.
[16] I. Koetschau, M.N. Richard, J.R. Dahn, J.B. Soupart, J.C. Rousche, J. Electrochem. Soc. 142 (1995) 2906.

[17] B. Ammundsen, J. Desilvestro, T. Groutso, D. Hassell, J.B. Metson, E. Regan, R. Steiner, P.J. Pickering, J. Electrochem. Soc. 147 (2000) 4078.
[18] J.M. Paulsen, C.L. Thomas, J.R. Dahn, J. Electrochem. Soc. 147 (2000) 861.
[19] T. Ohzuku, A. Ueda, J. Electrochem Soc. 141 (1994) 2972.
[20] T. Ohzuku, K. Nakura, T. Aoki, Electrochim. Acta 45 (1999) 151.
[21] T. Ohzuku, A. Ueda, M. Kouguchi, J. Electrochem. Soc. 142 (1995) 4033.